Drug Selectivity Is Determined by Coupling Across the NAD^+ Site of IMP Dehydrogenase†

Jennifer A. Digits and Lizbeth Hedstrom*

Department of Biochemistry, Brandeis University, Waltham, Massachusetts 02454

Received October 4, 1999; Revised Manuscript Received December 8, 1999

ABSTRACT: Drug resistance often results from mutations that are located far from the drug-binding site. The effects of these mutations are perplexing. The inhibition of IMPDH by MPA is an example of this phenomenon. Mycophenolic acid (MPA) is a species-specific inhibitor of IMPDH; mammalian IMPDHs are very sensitive to MPA, while the microbial enzymes are resistant to the inhibitor. MPA traps the covalent intermediate E-XMP* and binds in the nicotinamide half of the dinucleotide site. Previous results indicated that about half of the difference in sensitivity derives from residues in the MPA-binding site [Digits, J. A., and Hedstrom, L. (1999) *Biochemistry 38*, 15388−15397]. The remainder must be attributed to regions outside the MPA-binding site. The adenosine subsite of the NAD^+ site is not conserved among IMPDHs and is, therefore, a likely candidate. Our goal is to examine the coupling between the nicotinamide and adenosine sites in order to test this hypothesis. We performed multiple inhibitor experiments with the *Tritrichomonas foetus* and human type 2 IMPDHs using tiazofurin and ADP, which bind in the nicotinamide and adenosine subsites, respectively. For *T. foetus* IMPDH, tiazofurin and ADP are extraordinarily synergistic. In contrast, these inhibitors are virtually independent for the human type 2 enzyme. We suggest that the difference in coupling of the nicotinamide and adenosine subsites accounts for the remaining difference in MPA affinity between *T. foetus* and human IMPDH.

Drug resistance often results from mutations located outside the inhibitor binding pocket (*1*−*7*). The effects of these mutations are difficult to rationalize on structural grounds, since they do not play a direct role in inhibitor binding. In some cases, the mutations are believed to change the movement of flexible loops. For example, in HIV-1 protease, the Met46Ile mutation is associated with drug resistance. This mutation appears to stabilize the flap in a closed conformation (*4*, *6*). Similarly, in thymidylate synthase, two mutations involved in drug resistance, Asp49Gly and Gly52Ser, may impair the movement of a mobile loop (*3*). However, in many cases, the effects of the mutations are puzzling. For example, in HIV-1 protease, the Leu90Met mutation confers drug resistance, although Leu90 lies at the core of the protein with no obvious contact with the inhibitor (*5*).

Mycophenolic acid (MPA)[1] is an inhibitor of IMP dehydrogenase (IMPDH), the enzyme that catalyzes the rate-limiting step in de novo guanine nucleotide biosynthesis (Figure 1). MPA is a unique inhibitor, because it is species-specific; mammalian IMPDHs are very sensitive to MPA, while IMPDHs from most microbial sources are resistant to the inhibitor. For example, $K_i = 20$ nM for human IMPDH, 9 nM for Chinese hamster IMPDH, 0.2 μM for *Leishmania donovani* IMPDH, 9 μM for *Tritrichomonas foetus* IMPDH, and 20 μM for *Escherichia coli* IMPDH (*8*−*10*, Cahoon, M., and Hedstrom, L., unpublished results). Understanding the basis for this selectivity is important for the development of useful antimicrobial agents.

MPA inhibits IMPDH by trapping a covalent intermediate in the reaction, E-XMP*, and preventing hydrolysis (Figure 1) (*10*−*14*). In the crystal structure of the E-XMP*·MPA complex from Chinese hamster (98% identical to human type 2 IMPDH), MPA stacks against E-XMP* in the nicotinamide binding-site (*10*). This crystal structure identifies only two residues in the MPA-binding site, which are different in most microbial IMPDHs (*10*). Arg322 and Gln441 of the hamster IMPDH are replaced by Lys and Glu, respectively, in the microbial enzymes (Figure 2). Interestingly, IMPDH from *L. donovani* contains the Arg and Gln in the MPA-binding site as do mammalian IMPDHs, which could account for its partial sensitivity. Similarly, the Lys310Arg/Glu431Gln *T. foetus* mutant IMPDH has an inhibition constant for MPA that is only 20-fold lower than that of the wild-type enzyme (*9*). Thus, only 20 of the 450-fold difference in sensitivity between the *T. foetus* and human type 2 IMPDHs derives from the residues in the MPA-binding site. The remaining 23-fold must be attributed to regions outside the MPA-binding site.

Crystal structures of IMPDH from Chinese hamster, *T. foetus*, human type 2, and *Streptococcus pyogenes* show that

†Supported by NIH Molecular Structure and Function Training Grant GM07956 (J. A. D.), NIH GM54403 (L. H.), and a grant from the Markey Charitable Trust to Brandeis University.

* To whom correspondence should be addressed: Department of Biochemistry, Brandeis University MS 009, 415 South Street, Waltham, Massachusetts 02454. Telephone: (781) 736-2333. Fax: (781) 736-2349. E-mail: hedstrom@brandeis.edu.

[1] Abbreviations: IMPDH, inosine-5′-monophosphate dehydrogenase; IMP, inosine-5′-monophosphate; NAD^+, nicotinamide adenine dinucleotide; NADH, reduced nicotinamide adenine dinucleotide; XMP, xanthosine-5′-monophosphate; ADP, adenosine-5′-diphosphate; MPA, mycophenolic acid; TAD, thiazole-4-carboxamide adenine dinucleotide; β-Me-TAD, β-methylene thiazole-4-carboxamide adenine dinucleotide; tiazofurin, 2-β-D-ribofuranosylthiazole-4-carboxamide; DTT, dithiothreitol; SAD, selenazole-4-carboxamide adenine dinucleotide.

10.1021/bi992288e CCC: $19.00
Published on Web 01/28/2000

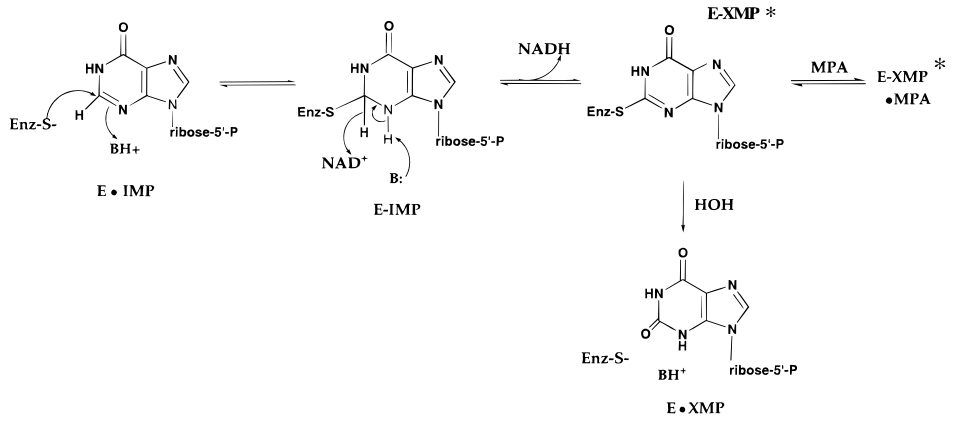

FIGURE 1: Mechanism of the IMPDH reaction.

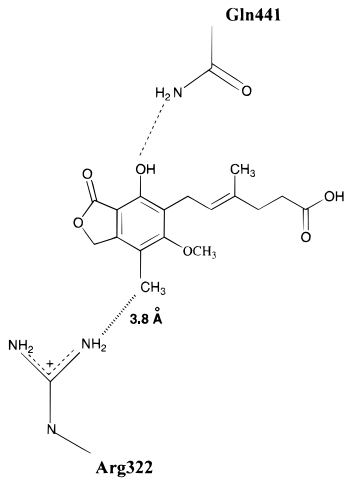

FIGURE 2: MPA and its interactions with Gln441 and Arg322 of Chinese hamster IMPDH.

the active site is composed of a long cleft containing an IMP-binding pocket contiguous with the NAD^+-binding groove (*10*, *15*−*17*). A flap (residues 400−450 in the human and hamster enzymes) covers the active site. The nucleophilic Cys is found in a mobile loop. While the residues of the IMP site are conserved among IMPDHs, the residues of the NAD^+ site are not. The NAD^+-binding groove and enzyme−cofactor interactions are defined by the presence of the NAD^+ analogue, SAD, in the structure of the human type 2 IMPDH (*16*). Here, the selenazole 4-carboxamide group occupies the nicotinamide pocket and stacks against the substrate analogue purine ring in a similar fashion as MPA. The adenosine end of the dinucleotide analogue binds in a cleft between two monomers. Interestingly, the adenosine end of the dinucleotide site is not conserved. Perhaps MPA resistance originates in the adenosine site.

In this study, we have performed multiple inhibitor experiments to investigate the coupling of the nicotinamide and adenosine subsites of the NAD^+ site. Our results indicate that the nicotinamide and adenosine subsites of the dinucleotide site are tightly coupled in the *T. foetus* IMPDH, but nearly independent in the human type 2 enzyme. Fluorescence studies with the *T. foetus* enzyme are consistent with this result. This difference in coupling across the NAD^+ site may account for the remaining difference in MPA affinity between *T. foetus* and human IMPDH.

MATERIALS AND METHODS

Materials. IMP, ADP, and Tris were purchased from Sigma. NAD^+ was purchased from Boehringer Mannheim. DTT was purchased from Research Organics, Inc. EDTA and KCl were purchased from Fisher. Tiazofurin was the gift of Dr. Victor Marquez (NCI). β-Me-TAD was the gift of Dr. Krzysztof W. Pankiewicz (Pharmasset, Inc.). Oligonucleotides were obtained from the Brandeis Oligonucleotide Facility.

Expression and Purification of IMPDH. Plasmids containing the IMPDH genes were purified from an *Escherichia coli* expression system using Cibacron blue affinity resin and cation exhange chromatography as previously described (*8*, *9*, *18*).

Mutagenesis. The *T. foetus* "Trp416" mutant was constructed from pTf1 using the Quikchange kit (Stratagene, La Jolla, CA). This mutant was constructed by producing a series of mutant IMPDHs in which the naturally occurring tryptophans were progresively replaced with phenylalanine residues. The resulting "Trp416" IMPDH contains only one native tryptophan at position 416 and has the following mutations: Trp190Phe/Trp269Phe/Trp276Phe/Trp406Phe. To ensure no undesired mutations had been introduced, the coding sequence of the IMPDH gene was sequenced using a PRISM Dyedeoxy Terminator Cycle Sequencing kit (Applied Biosystems, Inc.) and a 373A DNA sequencer at the Brandeis Sequencing Facility.

Enzyme Kinetics. Standard IMPDH assays contained 100 mM KCl, 3 mM EDTA, 1 mM DTT, and 50 mM Tris, pH 8.0 (assay buffer). The production of NADH was monitored spectrophotometrically at 340 nm ($\epsilon = 6.22\ mM^{-1}\ cm^{-1}$) at 25 °C using a Hitachi U-2000 spectrophotometer. The concentrations of IMP and NAD^+ or analog were varied for K_m determinations. Since substrate inhibition is observed, initial velocity data were fit to the Michaelis−Menten equation and uncompetitive substrate inhibition equation using Kaleidagraph software (Abelbeck Software) as described previously (*9*, *18*).

Inhibitor Kinetics. The values of K_i were determined in experiments containing constant, saturating IMP concentrations (150 μM) and varied NAD^+ concentrations. Multiple inhibition experiments with tiazofurin and ADP were performed with constant IMP and NAD^+ concentrations at 25 °C in assay buffer (substrate concentrations are contained in the Figure 4 legend).

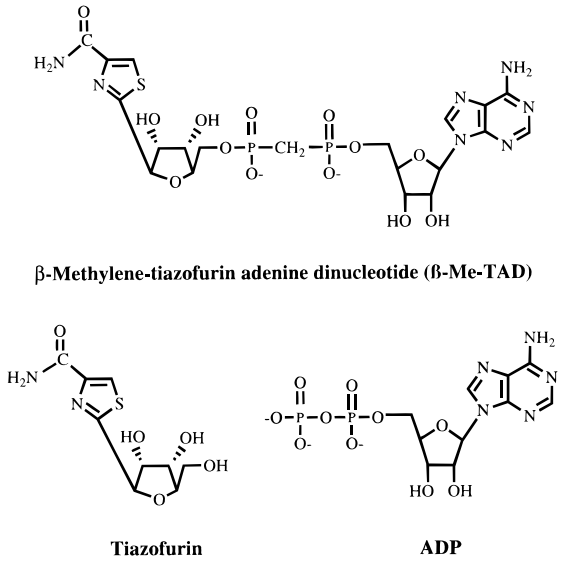

FIGURE 3: IMPDH inhibitors.

Data Analysis for Inhibition Studies. Initial rate data were fitted to eq 1−3 using KinetAsyst software II (Intellikinetics), and to eq 4 using Sigma Plot software (Jandel Scientific). The best fits were determined by the relative fit error.
competitive inhibition

$$v = V_m A/[K_a (1 + I/K_{is}) + A] \quad (1)$$

noncompetitive inhibition

$$v = V_m A/[K_a(1 + I/K_{is}) + A(1 + I/K_{ii})] \quad (2)$$

multiple inhibition

$$v = v_0/[1 + I/K_i + J/K_j + IJ/\alpha K_i K_j] \quad (3)$$

Ackermann−Potter noncompetitive tight binding inhibition

$$v = (v_0/2E)[(E - K_i - I) + (K_i + I + E)^2 - 4IE]^{0.5} \quad (4)$$

The nomenclature is that of Cleland (*19*): v is the velocity; V_m is the maximum velocity; A is the substrate concentration; K_a is the apparent Michaelis constant for A; K_{is} and K_{ii} are are the slope and intercept inhibition constants, respectively; I and J are the concentrations of inhibitors I and J; v_0 is the initial velocity in the absence of inhibitors I and J; α is the interaction constant between inhibitors I and J, and E is the enzyme concentration.

Fluorescence Spectroscopy. Equilibrium dissociation constants for the interaction of MPA and β-Me-TAD with the "Trp416" mutant *T. foetus* E·IMP complex were determined by following the quenching of intrinsic protein fluorescence. The measurements were performed on a Hitachi F-2000 fluorescence spectrophotometer at 25 °C. The excitation wavelength was 295 nm. Inner filter effects due to the MPA were corrrected as described previously (*9*, *18*). For binding of MPA and β-Me-TAD to the E·IMP complex, the enzyme was first incubated with saturating concentrations of IMP and then titrated with increasing concentrations of ligand. From the measured fluorescence intensity I at a given ligand concentration, fractional saturation of enzyme sites with ligand (f_a) was determined by using $f_a = (I - I_a)/(I_b - I_a)$, where I_a is the fluorescence of the apoenzyme, and I_b is the fluorescence of the enyzme when all of its binding sites are saturated with ligand. The free ligand concentration was estimated using $[\text{ligand}]_{free} = [\text{ligand}]_t - n[E]_t$, in which $[\text{ligand}]_t$ and $[E]_t$ represent the total ligand and apoenzyme

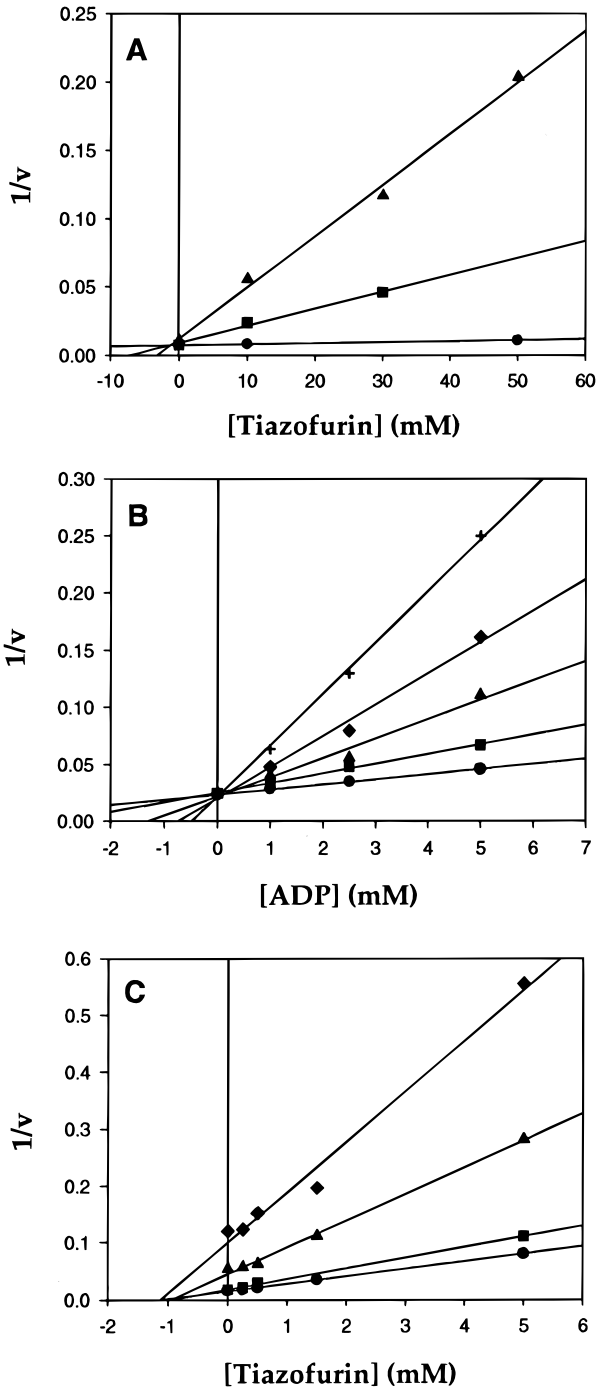

FIGURE 4: Multiple inhibition by tiazofurin and ADP. The reactions were performed under standard assay conditions as described in the Materials and Methods section. (A) $1/v$ vs [tiazofurin] plot for the wild-type *T. foetus* IMPDH. The concentration of IMP was 100 μM and that of NAD^+ was 500 μM. (●) No ADP; (■) 8 mM ADP; (▲) 20 mM ADP. (B) $1/v$ vs. [ADP] plot for the Lys310Arg/Glu431Gln enzyme. The concentration of IMP was 150 μM and that of NAD^+ was 400 μM. (●) No tiazofurin; (■) 1.5 mM tiazofurin; (▲) 4 mM tiazofurin; (◆) 8 mM tiazofurin; (+) 16 mM tiazofurin. (C) $1/v$ vs. [tiazofurin] plot for the human type 2 IMPDH. The concentration of IMP was 130 μM and that of NAD^+ was 30 μM. (●) No ADP; (■) 7.5 mM ADP; (▲) 30 mM ADP; (◆) 40 mM ADP.

Table 1: Multiple Inhibitor Experiments with Tiazofurin and ADP for Wild-type *T. Foetus*, Lys310Arg/Glu431Gln, and Human IMPDHs[a]

inhibitor	inhibition constant[b]	*T. foetus* wild-type IMPDH	Lys310Arg/Glu 431Gln IMPDH	human IMPDH
MPA	K_{ii} (UC)	$9 \pm 0.5\ \mu M$[c]	$0.5 \pm 0.04\ \mu M$[c]	$0.022 \pm 0.008\ \mu M$[d]
tiazofurin	K_{ii} (NC)	69 ± 9 mM[e]	≥75 mM	1.3 ± 0.1 mM
	K_{is} (NC)	50 ± 10 mM[e]	≥75 mM	4.2 ± 1.7 mM
β-Me-TAD	K_{ii} (NC)	$2.3 \pm 0.4\ \mu M$	$4.3 \pm 0.4\ \mu M$	$0.06 \pm 0.02\ \mu M$[f]
	K_{is} (NC)	$2.8 \pm 1.3\ \mu M$	$14 \pm 5\ \mu M$	
ADP	K_{is} (C)	31 ± 2 mM[e]	1.4 ± 0.3 mM	8.8 ± 2.2 mM
tiazofurin/ADP	α	0.007 ± 0.002	0.019 ± 0.005	1.3 ± 0.3

[a] Experimental conditions: 50 mM Tris, pH 8.0, 100 mM KCl, 3 mM EDTA, and 1 mM DTT at 25 °C. For single inhibitor experiments, the NAD^+ concentrations were varied and the IMP concentrations were fixed at 150 μM. [b] These are the inhibition constants and patterns vs NAD^+; C, competitive inhibition; NC, noncompetitive inhibition; UC, uncompetitive inhibition. [c] These values are from (*9*). [d] This value is from (*8*). [e] These values are from (*12*). [f] This value was obtained by fitting to the noncompetitive tight binding equation (eq 4).

concentration, respectively, and n is the number of ligand-binding sites on the enzyme ($n = 1$ for monomer concentration). Kaleidagraph software was used to fit f_a and $[ligand]_{free}$ to eq 5:

$$f_a = [ligand]_{free}/(K_d + [ligand]_{free}) \quad (5)$$

to give the dissociation constant, K_d.

RESULTS

Dead-End Inhibitors of IMPDH. The inhibition constants of MPA, tiazofurin, β-Me-TAD, and ADP are summarized in Table 1 (structures are in Figure 3). β-Me-TAD is a phosphodiesterase-resistant analogue of TAD, which has an identical inhibition constant to TAD for human type 2 IMPDH (*20*). The inhibition constant for the wild-type *T. foetus* enzyme is also similar to the value reported for TAD (*12*). β-Me-TAD is a noncompetitive inhibitor vs NAD^+ in all of the enzymes studied (Table 1). The inhibition constants for β-Me-TAD only differ by approximately 3-fold between the wild-type and mutant *T. foetus* IMPDHs. β-Me-TAD is a potent inhibitor of the human enzyme, with an inhibition constant ~40-fold lower than that of *T. foetus* IMPDH. Our value of $K_i = 0.06\ \mu M$ for human IMPDH is approximately 5-fold lower than other values reported in the literature (*20*−*22*). Under our experimental conditions, the concentration of enzyme is comparable to the concentrations of β-Me-TAD, which requires tight-binding inhibitor analysis, as described in the Materials and Methods section. Failure to account for tight-binding conditions, as may be the case in previous experiments, results in $K_i = 0.26\ \mu M$, comparable to the literature values.

Tiazofurin is a noncompetitive inhibitor vs NAD^+ for all of the enzymes (Table 1). It is a poor inhibitor of wild-type *T. foetus* IMPDH and a somewhat weaker inhibitor of the Lys310Arg/Glu431Gln enzyme, with inhibition constants in the high millimolar range. Tiazofurin is a much better inhibitor of human type 2 IMPDH, with an inhibition constant ~70-fold lower than those of the *T. foetus* enzymes.

ADP is a competitive inhibitor vs NAD^+ for all of the enzymes (Table 1). Surprisingly, ADP is a more potent inhibitor of the mutant enzyme than either of the wild-type IMPDHs. The inhibition constant for the mutant IMPDH is 20 and 6-fold lower than wild-type *T. foetus* and human IMPDHs, respectively.

Advantage of Connecting Tiazofurin and ADP. The inhibition constants for β-Me-TAD are much lower than those of either tiazofurin or ADP alone in all three enzymes studied, as expected, given that β-Me-TAD interacts simultaneously with both the nicotinamide and adenosine subsites (Table 1, Figure 3). The advantage of connecting tiazofurin and ADP as β-Me-TAD is equal to the ratio of dissociation constants, $(K_T K_{ADP})/K_{TAD}$ (*23*, *24*). Similarly, the binding energy of β-Me-TAD, ΔG_{TAD}, will be more favorable than $\Delta G_T + \Delta G_{ADP}$ by an amount equal to ΔG^S, a component of the free energy that represents the entropy loss upon binding β-Me-TAD (*23*). The advantage of combining tiazofurin and ADP to make β-Me-TAD is 200 M (3.2 kcal/mol), ≥30 M (≥2.0 kcal/mol), and 900 M (4.1 kcal/mol) for the human, mutant, and wild-type *T. foetus* enzymes, respectively. The advantage of binding β-Me-TAD to the mutant enzyme is a lower limit, since we only have a lower limit for the dissociation constant for tiazofurin. The advantage of connecting two sites can be as high as 10^8 M (12.4 kcal/mol) for an ideal case where the binding of the first component causes the second component to bind without further loss of entropy (*23*). Advantages of up to 5×10^4 M (6.5 kcal/mol) have been observed for compactin binding vs its component pieces to HMG-CoA reductase (*24*). In comparison, the advantage of binding TAD over tiazofurin and ADP is rather low. One explanation for this observation is that our component pieces are not ideal: tiazofurin and ADP overlap at the 5′-oxygen (Figure 3). Presumably, 5′-deoxytiazofurin will have a lower affinity than tiazofurin, which would increase the connectivity advantage.

Multiple Inhibition Studies. In a multiple inhibitor experiment, α is defined as the interaction constant (eq 3). If two inhibitors I and J bind mutually exclusively, $\alpha = \infty$, and the $1/v$ vs [J] plot at varied [I] is a series of parallel lines. If a ternary E−I−J complex can form, α must be between 0 and ∞. If $\alpha < 1$, I and J are synergistic, and if $\alpha > 1$, I and J are antagonistic. If $\alpha = 1$, the inhibitors are independent, which results in a pattern of lines intersecting on the [J] axis (*25*−*28*).

Previous results demonstrated that tiazofurin is mutually exclusive with NADH, but not with ADP, suggesting that tiazofurin binds in the nicotinamide portion of the NAD^+ site (*12*). Furthermore, MPA and tiazofurin are mutually exclusive, demonstrating that MPA binds in the tiazofurin, hence nicotinamide, portion of the NAD^+ site (*12*). This conclusion was confirmed in the crystal structure of the E-XMP*•MPA complex of Chinese hamster IMPDH (*10*).

To probe the coupling of the nicotinamide and adenosine subsites, multiple inhibitor experiments were performed with

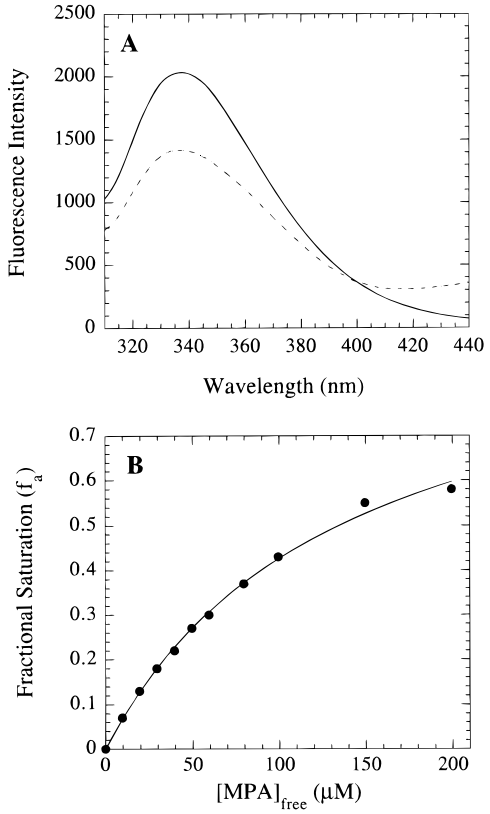

FIGURE 5: Binding of MPA to the "Trp416" *T. foetus* E·IMP complex. (A) Fluorescence emission spectra for "Trp416" E·IMP (solid line) and its complex with MPA (dashed line) when excited with light of 295 nm. The enzyme concentration is 2.0 μM, and that of MPA is 50 μM. (B) Dependence of fractional saturation of the enzyme on MPA concentration as E·IMP is titrated with increasing MPA. The data were fit to eq 5.

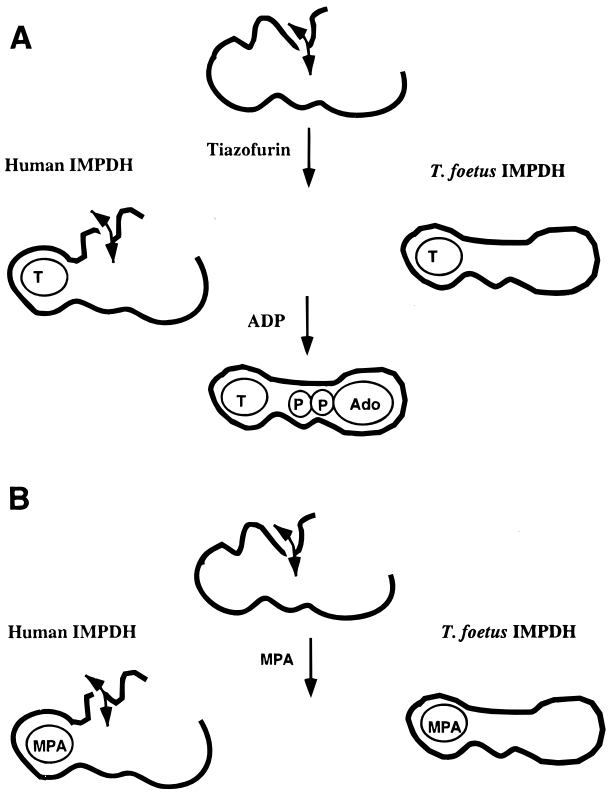

FIGURE 6: A model for the species-specific inhibition of MPA. (A) The nicotinamide and adenosine subsites are coupled in *T. foetus* IMPDH, but not in human IMPDH. In *T. foetus* IMPDH, the binding of tiazofurin orders the adenosine subsite. Therefore, the binding of ADP is synergistic. In human IMPDH, the binding of tiazofurin does not order the adenosine subsite. Therefore, the binding of ADP is independent. (B) Implications on MPA selectivity. In *T. foetus* IMPDH, the binding of MPA orders the adenosine subsite. Therefore, MPA binds with low affinity. In human IMPDH, the binding of MPA does not order the adenosine subsite. Thus, MPA binds with high affinity.

tiazofurin and ADP (Table 1, Figure 4). For the wild-type *T. foetus* IMPDH, the interaction of tiazofurin with ADP is strongly synergistic, with an $\alpha = 0.007$. Figure 4A shows the $1/v$ vs [tiazofurin] plot, with a pattern of lines intersecting on the $1/v$ axis. Similar results with the *T. foetus* enzyme were obtained previously (*12*). For the *T. foetus* mutant enzyme, the interaction of tiazofurin with ADP is also synergistic, with an $\alpha = 0.019$ (Table 1, Figure 4B). However, essentially no interaction exists between tiazofurin and ADP for the human type 2 IMPDH (Table 1, Figure 4C). The value of α is 1.3.

Fluorescence Spectroscopy: *the "Trp416" Mutant IMPDH*. To further probe the adenosine subsite of *T. foetus* IMPDH, the single tryptophan mutant "Trp416" was constructed as described in the Methods section. "Trp416" designates the mutant containing only one tryptophan at position 416 in the flap region of IMPDH. "Trp416" IMPDH exhibits wild-type activity and has the following steady-state kinetic parameters: $k_{cat} = 0.93\ s^{-1}$, K_m (IMP) = 5.6 μM, and K_m (NAD^+) = 72 μM.

The single tryptophan residue, Trp416, can be selectively excited at 295 nm. The association of β-Me-TAD with the "Trp416" E·IMP complex quenches the protein fluorescence (data not shown). Similarly, the binding of MPA to "Trp416" E·IMP causes a decrease in the fluorescence intensity of the enzyme. As shown in Figure 5A, MPA at a concentration of 50 μM quenches the protein fluorescence by 28%. The value of the dissociation constants (K_d) for ligand binding can be determined from the dependence of fluorescence intensity upon ligand concentration. Figure 5B showns a binding curve in which the changes in fluorescence are represented by fractional saturation of enzyme sites with MPA as its concentration increases. The dissociation constants measured in this way are 3.7 and 136 μM for the association of β-Me-TAD and MPA, respectively, to the "Trp416" E·IMP complex.

DISCUSSION

MPA is a uniquely species-specific inhibitor of IMPDH. Much of this specificity must derive from distal structural elements since both *L. donovani* and the *T. foetus* Lys310Arg/Glu431Gln mutant IMPDHs are only partially sensitive to MPA. We performed multiple inhibitor experiments to examine the coupling between the nicotinamide and adenosine subsites in MPA-sensitive and MPA-resistant IMPDHs.

Tiazofurin and ADP are synergistic in the wild-type *T. foetus* IMPDH, but completely independent in the human type 2 enzyme (Table 1, Figure 4). These results indicate that the nicotinamide and adenosine subsites are tightly coupled in *T. foetus* IMPDH, but not in human IMPDH. Figure 6A shows one possible model that can account for these observations. The dinucleotide site is disordered in the absence of ligand in both enzymes (*10*, *15*−*17*). In *T. foetus*

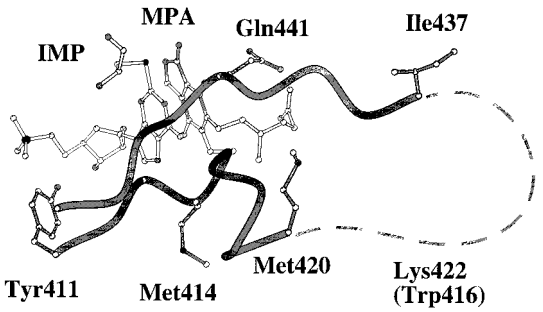

FIGURE 7: The active site of Chinese hamster IMPDH (*10*). The IMP is shown in white and its hypoxanthine ring makes a covalent bond to the sulfur of Cys331. The MPA is shown in light gray and makes a stacking interaction with the hypoxanthine ring. The "proximal" section of the active site flap is shown in dark gray. The side chains of selected residues that interact with IMP and MPA are also shown in dark gray: Tyr411, Met414, Gly415, and Gln441 (human and hamster IMPDH numbering). The "terminal" loop of the flap, which is disordered in this structure, is designated by the dotted line. The corresponding residue in the *T. foetus* enzyme is in parentheses. This figure was produced using MOLSCRIPT (*29*).

IMPDH, the binding of tiazofurin orders the adenosine subsite, thus increasing the affinity for ADP. In contrast, in the human IMPDH, binding of ADP is independent of tiazofurin, because the binding of tiazofurin does not order the adenosine subsite.

Implications for MPA Selectivity. Similarly, when MPA binds to *T. foetus* IMPDH, it may order the adenosine subsite. As a consequence, MPA binds with low affinity, because some of the intrinsic binding energy is lost in ordering the adenosine subsite. However, when MPA binds to human IMPDH, it does not order the adenosine subsite and, therefore, binds with high affinity, because all of the intrinsic binding energy is expressed in binding (Figure 6B).

This model is supported by the crystal structure of E-XMP*·MPA from Chinese hamster (*10*) (Figure 7). While MPA binds in the nicotinamide subsite, the adenosine subsite is empty in this complex. IMP and MPA make interactions with several residues from the "proximal" portion of the flap: Tyr411, Met414, Gly415, and Gln441 (human IMPDH numbering; Figure 7). In the presence of a dinucleotide ligand, the adenosine subsite is covered by the "terminal" portion of flap, comprising residues 420−437 (*16*). The "terminal" flap loop is disordered in this structure (Figure 7). Thus, the binding of MPA in human IMPDH does not involve an interaction with the "terminal" loop. Interestingly, the residues comprising this loop are not conserved among IMPDHs.

Unfortunately, there is no structure of E-XMP*·MPA from *T. foetus* IMPDH. Our model predicts that the "terminal" flap loop will be ordered in this complex, and that the energy required to drive this loop movement will decrease the observed MPA-binding energy. To test this hypothesis, we performed a fluorescence experiment with the *T. foetus* "Trp416" mutant IMPDH. Residue Trp416 corresponds with Lys422 of the human enzyme and is in the "terminal" flap loop, most likely near the adenosine ribose and phosphate moiety (Figure 7). If the conformation of Trp416 changes in response to ligand binding, then its fluorescence properties should also change. We examined the binding of ligands to the E·IMP complex instead of E-XMP*, since E-XMP* is not stable. The association of β-Me-TAD to the "Trp416" E·IMP complex causes the fluorescence to decrease (not shown), which is expected, since crystallographic data indicate that the presence of a dinucleotide orders the "terminal" flap loop (*16*).

Similarly, the binding of MPA to the nicotinamide subsite of the "Trp416" E·IMP complex causes the protein fluorescence to decrease (Figure 5A). Although the mechanism of protein fluorescence quenching is complex, these results indicate that the environment of Trp416 changes in response to MPA binding, which implies that the "terminal" loop may become ordered in the E·IMP·MPA complex. Since Trp416 is not in close vicinity to MPA (Figure 7), these results suggest that the association of MPA with *T. foetus* IMPDH is "coupled" to movement of the "terminal" flap loop. These fluorescence observations are consistent with the model proposed above, although more structural data are necessary to be definitive.

The Lys310Arg/Glu431Gln *T. foetus* enzyme exhibits almost identical behavior to the wild-type *T. foetus* enzyme (Table 1, Figure 4). However, the value of α is ~3-fold larger than that of the wild-type *T. foetus* enzyme, as if there is a small degree of uncoupling between the nicotinamide and adenosine subsites. Since the value of α is still 70-fold smaller than that of human IMPDH, the residues in the MPA-binding site do not control the coupling between the nicotinamide and adenosine subsites.

Interestingly, these two residues change the distribution of binding energies in the NAD^+ site. While the K_i of β-Me-TAD for the mutant enzyme is very similar to that of the wild-type *T. foetus* enzyme, the K_i of tiazofurin increases, and the K_i of ADP decreases (Table 1). This observation is consistent with our coupling model. As discussed by Jencks (*23*), the total, or intrinsic binding energy of tiazofurin to IMPDH, ΔG_{ibe}, is the sum of the observed binding energy, ΔG_{obs}, and the interaction energy, ΔG_{int} (eq 6):

$$\Delta G_{ibe} = \Delta G_{obs} + \Delta G_{int} \quad (6)$$

In our case, ΔG_{int} represents the coupling energy used to induce conformational changes in the adenosine subsite caused by the presence of tiazofurin in the nicotinamide subsite. In the human enzyme, these two sites are independent. Therefore, ΔG_{ibe} for tiazofurin binding is equal to ΔG_{obs} (−4.0 kcal/mol). For wild-type *T. foetus* IMPDH, where the two sites are coupled, $\Delta G_{ibe} = -4.6$ kcal/mol ($\Delta G_{int} = -3.0$ kcal/mol and $\Delta G_{obs} = -1.6$ kcal/mol). Thus, the ΔG_{ibe} is greater in the *T. foetus* enzyme, although the K_i of tiazofurin is lower in the human enzyme. While the Lys310Arg/Glu431Gln *T. foetus* enzyme also displays strong coupling between the nicotinamide and adenosine subsites, the K_i of tiazofurin increases. The resulting value of $\Delta G_{ibe} = -3.95$ kcal/mol is equivalent to the human enzyme, as expected, since the structures of the nicotinamide-binding sites are identical.

The K_i of ADP is much lower for the mutant *T. foetus* enzyme than in wild-type *T. foetus* IMPDH (Table 1). The mutations may interact with the β-phosphate of ADP, which could account for this observation (the carboxylic acid group of MPA may overlap with the β-phosphate of ADP). The inhibition constant for ADP should differ from the human enzyme, since the adenosine sites are not conserved.

The difference in coupling between the nicotinamide and adenosine subsites in the Lys310Arg/Glu431Gln and human enzymes may determine MPA selectivity. The 23-fold difference in the inhibition constants between the mutant and human enzymes corresponds to an energy difference in binding of 1.9 kcal/mol. Assuming that MPA binding couples to the adenosine site as observed with tiazofurin, then $\Delta G_{int} = -2.4$ kcal/mol for the double mutant enzyme vs 0 for human IMPDH. Therefore, this difference in interaction energy can account for the remaining differences in MPA sensitivity between the *T. foetus* and human type 2 IMPDHs.

ACKNOWLEDGMENT

We would like to thank Dr. Chris Miller for his helpful comments on the manuscript, Dr. Carin Stamper for her assistance with the MPA structure figure, and Rebecca Taurog for her technical assistance with the "Trp416" mutant IMPDH. We also thank Michael Sintchak and Dr. Barry Goldstein for generously providing coordinates for the Chinese hamster and human type 2 IMPDHs, respectively.

REFERENCES

1. Kaplan, A. H., Michael, S. F., Wehbie, R. S., Knigge, M. F., Paul, D. A., Everitt, L., Kempf, D. J., Norbeck, D. W., Erickson, J. W., and Swanstrom, R. (1994) *Proc. Natl. Acad. Sci. U.S.A. 91*, 5597−5601.
2. Smidt, M. L., Potts, K. E., Tucker, S. P., Blystone, L., Stiebel, T. R., Stallings, W. C., McDonald, J. J., Pillay, D., Richman, D. D, and Bryant, M. L. (1997) *Antimicrob. Agents Chemother. 41*, 515−522.
3. Tong, Y., Liu-Chen, X., Ercikan-Abali, E. A., Capiaux, G. M., Zhao, S., Banerjee, D., and Bertino, J. R. (1998) *J. Biol. Chem. 273*, 11611−11618.
4. Ho, D. D., Toyoshima, T. Hongmei, M., Kempf, D. J., Norbeck, D., Chen, C., Wideburg, N. E., Burt, S. K., Erickson, J. W., and Singh, M. K. (1994) *J. Virol. 68*, 2016−2020.
5. Jacobsen, H., Yasargil, K., Winslow, D. L., Craig, J. C., Krohn, A., Duncan, I. B., and Mous, J. (1995) *Virology 206*, 527−534.
6. Collins, J. R., Burt, S. K., and Erickson, J. W. (1995) *Struct. Biol. 2*, 334−338.
7. Erickson, J. W. (1995) *Nat. Struct. Biol. 2*, 523−529.
8. Farazi, T., Leichman, J., Harris, T., Cahoon, M., and Hedstrom, L. (1997) *J. Biol. Chem. 272*, 961−965.
9. Digits, J. A., and Hedstrom, L. (1999) *Biochemistry 38*, 15388−15397.
10. Sintchak, M. D., Fleming, M. A., Futer, O., Raybuck, S. A., Chambers, S. P., Caron, P. R., Murcko, M. A., and Wilson, K. P. (1996) *Cell 85*, 921−930.
11. Link, J. O., and Straub, K. (1996) *J. Am. Chem. Soc. 118*, 2091−2092.
12. Hedstrom, L., and Wang, C. C. (1990) *Biochemistry 29*, 849−554.
13. Wu, J. C., Carr, S. F., Antonino, L. C., Papp, E., and Pease, J. H. B. (1995) *FASEB Abstr. 9*, 472.
14. Fleming, M. A., Chambers, S. P., Connelly, P. R., Nimmersgen, E., Fox, T., Bruzzese, F. J., Hoe, F. J., Fulghem, J. R., Livingston, D. J., Stuver, C. M., Sintchak, M. D., Wilson, K. P., and Thomson, J. A. (1996) *Biochemistry 35*, 6990−6997.
15. Whitby, F. G., Luecke, H., Kuhn, P., Somoza, J. R., Huete-Perez, J. A., Phillips, J. D., Hill, C. P., Fletterick, R. J., and Wang, C. C. (1997) *Biochemistry 36*, 10666−10674.
16. Colby, T. D., Vanderveen, K., Strickler, M. D., Markham, G. D., and Goldstein, B. M. (1999) *Proc. Natl. Acad. Sci. U.S.A. 96*, 3531−3536.
17. Zhang, R., Evans, G., Rotella, F. J., Westbrook, E. M., Beno, D., Huberman, E., Joachimiak, A., and Collart, F. R. (1999) *Biochemistry 38*, 4691−4700.
18. Digits, J. A., and Hedstrom, L.(1999) *Biochemistry 38*, 2295−2306.
19. Cleland, W. W. (1963) *Biochim. Biophys. Acta 67*, 104−137.
20. Marquez, V. E., Tseng, C. K. H., Gebeyehu, G., Cooney, D. A., Ahluwalia, G. S., Kelley, J. A., Dalal, M., Fuller, R. W., Wilson, Y. A., and Johns, D. G. (1986) *J. Med. Chem. 29*, 1726−1731.
21. Hager, R. W., Collart, F. R., Huberman, E., and Mitchell, B. S. (1995) *Biochem. Pharmacol. 49*, 1323−1329.
22. Yamada, Y., Natsumeda, Y., and Weber, G. (1988) *Biochemistry 27*, 2193-2196.
23. Jencks, W. P. (1981) *Proc. Natl. Acad. Sci. U.S.A. 78*, 4046−4050.
24. Nakamura, C. E., and Abeles, R. H. (1985) *Biochemistry 24*, 1364−1376.
25. Schimerlik, M. I., and Cleland, W. W. (1977) *Biochemistry 16*, 565−570.
26. Northrop, D. B., and Cleland, W. W. (1974) *J. Biol. Chem. 249*, 2928−2931.
27. Cleland, W. W. (1977) *Adv. Enzymol. Relat. Areas Mol. Biol. 45*, 273−387.
28. Yonetani, T., and Theorell, H. (1964) *Arch. Biochem. Biophys. 106*, 2193-2196.
29. Kraulis, P. J. (1991) *J. Appl. Crystallogr. 24*, 946−950.

BI992288E